Nucleon electromagnetic form factors with a nonlocal chiral effective Lagrangian

Fangcheng He[1,2] and P. Wang[1,3]
[1]*Institute of High Energy Physics, CAS, P. O. Box 918(4), Beijing 100049, China*
[2]*University of Chinese Academy of Sciences, Beijing 100049, China*
[3]*Theoretical Physics Center for Science Facilities, CAS, Beijing 100049, China*

(Received 16 November 2017; published 12 February 2018)

The relativistic version of finite-range regularization is proposed. The covariant regulator is generated from the nonlocal Lagrangian. This nonlocal interaction is gauge invariant and is applied to study the nucleon electromagnetic form factors at momentum transfer up to 2 GeV^2. Both octet and decuplet intermediate states are included in the one-loop calculation. Using a dipole regulator with Λ around 0.85 GeV, the obtained form factors, electromagnetic radii, as well as the ratios of the form factors are all comparable with the experimental data. This successful application of chiral effective Lagrangian to relatively large momentum transfer makes it possible to further investigation of hadron quantities at high Q^2.

DOI: 10.1103/PhysRevD.97.036007

I. INTRODUCTION

The study of the properties of hadrons continues to attract significant interest in the process of revealing and understanding the essential mechanisms of the strong interactions. The investigation of the electromagnetic form factors of the nucleon is very important to help us discover their internal structure. Though QCD is the fundamental theory to describe strong interactions, it is difficult to study hadron physics using QCD directly. There are many phenomenological models, such as the cloudy bag model [1], the constituent quark model [2,3], the $1/N_c$ expansion approach [4], the perturbative chiral quark model [5], the extended vector meson dominance model [6], the SU(3) chiral quark model [7], the quark-diquark model [8,9], etc.

Besides the phenomenological models, there are also many lattice-QCD calculations for the electromagnetic form factors [10–16]. Lattice simulation is the most rigorous approach that starts from the first principles. Because of the computing limit, most quantities are still calculated with large quark (π) mass.

In hadron physics, another important method is chiral perturbation theory (ChPT). Heavy baryon and relativistic chiral perturbation theory have been widely applied to study the hadron spectrum and structure. Historically, most formulations of ChPT have been based on dimensional or infrared regularization. Though ChPT is a successful and systematic approach, for the nucleon electromagnetic form factors, it is only valid for $Q^2 < 0.1\ \mathrm{GeV}^2$ [17]. When vector mesons are included, the result is close to the experiments with Q^2 less than 0.4 GeV^2 [18]. Therefore, with traditional ChPT, it is hard to study the form factors at relatively large Q^2, for example, to explain the G_E/G_M puzzle at large Q^2.

An alternative regularization method, namely, finite-range regularization (FRR), has been proposed. Inspired by quark models that account for the finite size of the nucleon as the source of the pion cloud, effective field theory with FRR has been widely applied to extrapolate the vector meson mass, magnetic moments, magnetic form factors, strange form factors, charge radii, first moments of generalized parton distributions, nucleon spin, etc. [19–34]. In the finite-range regularization, there is no cut for the energy integral. The regulator is not covariant and is in three-dimensional momentum space. This nonrelativistic regulator can only be applied with the heavy baryon ChPT. A lot of investigations have been done for the finite-range regularization and we have good knowledge on the nonrelativistic regulator that was kept the same for all the above calculations. But we know little about the relativistic regulator and we try to determine the relativistic regulator from the well-known form factors of nucleon.

In this paper, we provide a relativistic version of FRR. If we simply replace the nonrelativistic regulator with a covariant one, the local gauge symmetry and charge conservation is destroyed. As a result, the renormalized proton (neutron) charge is not 1 (0). Therefore, we generate the covariant regulator from the local gauge invariant Lagrangian. As a result, the nonlocal Lagrangian is introduced. Using this nonlocal chiral effective Lagrangian, we study the electromagnetic form factors up to $Q^2 = 2\ \mathrm{GeV}^2$. The paper is organized in the following way. In Sec. II, we briefly introduce the chiral Lagrangian and construct the nonlocal interactions. The matrix elements of the nucleon electromagnetic current are derived in Sec. III. Numerical results are presented in Sec. IV. Finally, Sec. V is a summary.

II. CHIRAL EFFECTIVE LAGRANGIAN

The lowest order chrial Lagrangian for baryons, pseudoscalar mesons, and their interaction can be written as [35,36]

$$\mathcal{L} = i\mathrm{Tr}\bar{B}\gamma_\mu \not{D} B - m_B \mathrm{Tr}\bar{B}B + \bar{T}^{abc}_\mu (i\gamma^{\mu\nu\alpha}D_\alpha - m_T\gamma^{\mu\nu})T^{abc}_\nu + \frac{f^2}{4}\mathrm{Tr}\partial_\mu\Sigma\partial^\mu\Sigma^+ + D\mathrm{Tr}\bar{B}\gamma_\mu\gamma_5\{A_\mu, B\} + F\mathrm{Tr}\bar{B}\gamma_\mu\gamma_5[A_\mu, B] + \left[\frac{\mathcal{C}}{f}\epsilon^{abc}\bar{T}^{ade}_\mu(g^{\mu\nu} + z\gamma_\mu\gamma_\nu)B^e_c\partial_\nu\phi^d_b + \mathrm{H.C}\right], \tag{1}$$

where D, F, and $\mathcal{C}$ are the coupling constants. The chiral covariant derivative $\mathcal{D}_\mu$ is defined as $\mathcal{D}_\mu B = \partial_\mu B + [V_\mu, B]$. The pseudoscalar meson octet couples to the baryon field through the vector and axial vector combinations as

$$V_\mu = \frac{1}{2}(\zeta\partial_\mu\zeta^\dagger + \zeta^\dagger\partial_\mu\zeta) + \frac{1}{2}ie\mathcal{A}^\mu(\zeta^+ Q\zeta + \zeta Q\zeta^+),$$
$$A_\mu = \frac{1}{2}(\zeta\partial_\mu\zeta^\dagger - \zeta^\dagger\partial_\mu\zeta) - \frac{1}{2}e\mathcal{A}^\mu(\zeta Q\zeta^+ - \zeta^+ Q\zeta), \tag{2}$$

where

$$\zeta = e^{i\phi/f}, \qquad f = 93 \text{ MeV}. \tag{3}$$

The matrix of pseudoscalar fields ϕ is expressed as

$$\phi = \frac{1}{\sqrt{2}}\begin{pmatrix} \frac{1}{\sqrt{2}}\pi^0 + \frac{1}{\sqrt{6}}\eta & \pi^+ & K^+ \\ \pi^- & -\frac{1}{\sqrt{2}}\pi^0 + \frac{1}{\sqrt{6}}\eta & K^0 \\ K^- & \bar{K}^0 & -\frac{2}{\sqrt{6}}\eta \end{pmatrix}. \tag{4}$$

$\mathcal{A}^\mu$ is the photon field. The covariant derivative D_μ in the decuplet part is defined as $D_\nu T^{abc}_\mu = \partial_\nu T^{abc}_\mu + (\Gamma_\nu, T_\mu)^{abc}$, where Γ_ν is the chrial connection [37] defined as $(X, T_\mu) = (X)^a_d T^{dbc}_\mu + (X)^b_d T^{adc}_\mu + (X)^c_d T^{abd}_\mu$. $\gamma^{\mu\nu\alpha}$,$\gamma^{\mu\nu}$ are the antisymmetric matrices expressed as

$$\gamma^{\mu\nu} = \frac{1}{2}[\gamma^\mu, \gamma^\nu] \quad \text{and} \quad \gamma^{\mu\nu\rho} = \frac{1}{4}\{[\gamma^\mu, \gamma^\nu], \gamma^\rho\}. \tag{5}$$

In the chiral $SU(3)$ limit, the octet and decuplet baryons have the same mass m_B and m_T. In our calculation, we use the physical masses for baryon octets and decuplets. The explicit form of the baryon octet is written as

$$B = \begin{pmatrix} \frac{1}{\sqrt{2}}\Sigma^0 + \frac{1}{\sqrt{6}}\Lambda & \Sigma^+ & p \\ \Sigma^- & -\frac{1}{\sqrt{2}}\Sigma^0 + \frac{1}{\sqrt{6}}\Lambda & n \\ \Xi^- & \Xi^0 & -\frac{2}{\sqrt{6}}\Lambda \end{pmatrix}. \tag{6}$$

For the baryon decuplets, there are three indices, defined as

$$T_{111} = \Delta^{++}, \qquad T_{112} = \frac{1}{\sqrt{3}}\Delta^+, \qquad T_{122} = \frac{1}{\sqrt{3}}\Delta^0,$$
$$T_{222} = \Delta^-, \qquad T_{113} = \frac{1}{\sqrt{3}}\Sigma^{*,+}, \qquad T_{123} = \frac{1}{\sqrt{6}}\Sigma^{*,0},$$
$$T_{223} = \frac{1}{\sqrt{3}}\Sigma^{*,-}, \qquad T_{133} = \frac{1}{\sqrt{3}}\Xi^{*,0}, \qquad T_{233} = \frac{1}{\sqrt{3}}\Xi^{*,-},$$
$$T_{333} = \Omega^-. \tag{7}$$

The octet, decuplet, and octet-decuplet transition magnetic moment operators are needed in the one-loop calculation of nucleon electromagnetic form factors. The baryon octet anomalous magnetic Lagrangian is written as

$$\mathcal{L} = \frac{e}{4m_N}(c_1\mathrm{Tr}\bar{B}\sigma^{\mu\nu}\{F^+_{\mu\nu}, B\} + c_2\mathrm{Tr}\bar{B}\sigma^{\mu\nu}[F^+_{\mu\nu}, B]), \tag{8}$$

where

$$F^+_{\mu\nu} = -\frac{1}{2}(\zeta^\dagger F_{\mu\nu}Q\zeta + \zeta F_{\mu\nu}Q\zeta^\dagger). \tag{9}$$

The transition magnetic operator is

$$\mathcal{L} = i\frac{e}{4m_N}\mu_T F_{\mu\nu}(\epsilon_{ijk}Q^i_j\bar{B}^j_m\gamma^\mu\gamma_5 T^{\nu,klm} + \epsilon^{ijk}Q^l_i\bar{T}^\mu_{klm}\gamma^\nu\gamma_5 B^m_j), \tag{10}$$

where the matrix Q is defined as $Q = \mathrm{diag}\{2/3, -1/3, -1/3\}$. At the lowest order, the Lagrangian generates the following nucleon anomalous magnetic moments:

$$F^p_2 = \frac{1}{3}c_1 + c_2, \qquad F^n_2 = -\frac{2}{3}c_1. \tag{11}$$

In the quark model, the nucleon magnetic moments can be written in terms of quark magnetic moments. For example, $\mu_p = \frac{4}{3}\mu_u - \frac{1}{3}\mu_d$, $\mu_n = \frac{4}{3}\mu_d - \frac{1}{3}\mu_u$. Using $\mu_u = -2\mu_d = -2\mu_s$, we can get the following relationships:

$$c_1 = \frac{3}{2}(c_2 + 1), \qquad c_1 = \frac{3}{2}\mu_u, \qquad \mu_T = 4c_1. \tag{12}$$

The effective decuplet anomalous magnetic moment operator can be expressed as effective Lagrangian

$$\mathcal{L} = \frac{ieF^T_2}{2m_T}\bar{T}^{abc}_\mu\sigma^{\rho\sigma}q_\sigma\mathcal{A}_\rho T^{abc}_\mu. \tag{13}$$

For each decuplet baryon, its moment F^T_2 can be written in terms of c_1. For example, for Δ^{++}, the magnetic moment $\mu_{\Delta^{++}} = 3\mu_u = 2c_1$. Therefore, $F^{\Delta^{++}}_2 = 2c_1 - 2$. In our numerical calculations, the above anomalous magnetic moments of baryons at tree level that only depend on the parameter c_1 are used.

Now we construct the nonlocal Lagrangian that generates the covariant regulator. The gauge invariant nonlocal Lagrangian can be obtained using the method in [38–40]. For instance, the local interaction including π meson can be written as

$$\mathcal{L}_\pi{}^{\mathrm{local}} = \int dx \frac{D+F}{\sqrt{2}f}\bar{p}(x)\gamma^\mu\gamma_5 n(x)(\partial_\mu + ie\mathcal{A}_\mu(x))\pi^+(x). \tag{14}$$

The nonlocal Lagrangian for this interaction is expressed as

$$\begin{aligned}\mathcal{L}_\pi{}^{nl} = &\int dx\int dy \frac{D+F}{\sqrt{2}f}\bar{p}(x)\gamma^\mu\gamma_5 n(x)F(x-y)\\ &\times \exp\left[ie\int_x^y dz_\nu \int da\mathcal{A}^\nu(z-a)F(a)\right]\\ &\times\left(\partial_\mu + ie\int da\mathcal{A}_\mu(y-a)F(a)\right)\pi^+(y),\end{aligned} \tag{15}$$

where $F(x)$ is the correlation function. To guarantee the gauge invariance, the gauge link is introduced in the above Lagrangian. The regulator can be generated automatically with correlation function. As in Ref. [38], we introduce the notation

$$I(x,y,p) \equiv \int_x^y dz_\nu \int da\mathcal{A}^\nu(z-a)F(a), \tag{16}$$

where p explicitly denotes the dependence on the path from x to y. The derivative is defined by

$$\lim_{dy_\mu\to 0} dy_\mu \frac{\partial}{\partial y^\mu}I(x,y,p) = \lim_{dy_\mu\to 0} I(x,y,+dy_\mu,p') - I(x,y,p), \tag{17}$$

where the path p' is the same as p except adding the extension dy_μ to the y end. With the definition in the above equation, we have

$$\frac{\partial}{\partial y^\mu}I(x,y,p) = \int da\mathcal{A}_\mu(y-a)F(a). \tag{18}$$

The important point is that the derivative of the path integral does not depend on the path used in defining it.

With the same idea, the nonlocal electromagnetic interaction can also be obtained. For example, the local interaction between proton and photon is written as

$$\begin{aligned}\mathcal{L}_{\mathrm{EM}}^{\mathrm{local}} = &-e\bar{p}(x)\gamma^\mu p(x)\mathcal{A}_\mu(x)\\ &-\frac{(c_1-1)e}{4m_N}\bar{p}(x)\sigma^{\mu\nu}p(x)F_{\mu\nu}(x).\end{aligned} \tag{19}$$

The corresponding nonlocal Lagrangian is expressed as

$$\begin{aligned}\mathcal{L}_{\mathrm{EM}}^{nl} = &-e\int da\bar{p}(x)\gamma^\mu p(x)\mathcal{A}_\mu(x-a)F_1(a)\\ &-\frac{(c_1-1)e}{4m_N}\int da\bar{p}(x)\sigma^{\mu\nu}p(x)F_{\mu\nu}(x-a)F_2(a),\end{aligned} \tag{20}$$

where $F_1(a)$ and $F_2(a)$ is the correlation function for the nonlocal electric and magnetic interactions. The form factors at tree level that are momentum dependent can be easily obtained with the Fourier transformation. The simplest choice is to assume that the correlation function of the nucleon electromagnetic vertex is the same as that of the nucleon-pion vertex, i.e., $F_1(a) = F_2(a) = F(a)$. Therefore, the Dirac and Pauli form factors have the same dependence on the momentum transfer at tree level. As a result, the obtained charge form factor of the proton decreases very quickly with increasing Q^2 and it becomes negative after some Q^2. The better choice is to assume that the charge and magnetic form factors at tree level have the same the momentum dependence as the nucleon-pion vertex, i.e., $G_M^{\mathrm{tree}}(p) = c_1 G_E^{\mathrm{tree}}(p) = c_1\tilde{F}(p)$, where $\tilde{F}(p)$ is the Fourier transformation of the correlation function $F(a)$. The corresponding function of $\tilde{F}_1(q)$ and $\tilde{F}_2(q)$ is then expressed as

$$\tilde{F}_1^p(q) = \tilde{F}(q)\frac{4m_N^2 + c_1Q^2}{4m_N^2+Q^2}, \qquad \tilde{F}_2^p(q) = \tilde{F}(q)\frac{4m_N^2}{4m_N^2+Q^2}. \tag{21}$$

From the above equations, one can see that in the heavy baryon limit, these two choices are equivalent. The nonlocal Lagrangian is invariant under the following gauge transformation,

$$\begin{aligned}&\pi^+(y) \to e^{i\alpha(y)}\pi^+(y), \qquad p(x) \to e^{i\alpha(x)}p(x),\\ &\mathcal{A}_\mu(x) \to \mathcal{A}_\mu(x) - \frac{1}{e}\partial_\mu\alpha'(x),\end{aligned} \tag{22}$$

where $\alpha(x) = \int da\alpha'(x-a)F(a)$. From Eq. (15), two kinds of couplings between hadrons and one photon can be obtained. One is the normal interaction expressed as

$$\begin{aligned}\mathcal{L}^{\mathrm{nor}} = ie&\int dx\int dy\frac{D+F}{\sqrt{2}f}\bar{p}(x)\gamma^\mu\gamma_5 n(x)F(x-y)\pi^+(y)\\ &\times\int da\mathcal{A}_\mu(y-a)F(a).\end{aligned} \tag{23}$$

This interaction is similar to the traditional local Lagrangian except the correlation function. The other one is the additional interaction obtained by the expansion of the gauge link, expressed as

$$\mathcal{L}^{\rm add} = ie\int dx\int dy\frac{D+F}{\sqrt{2}f}\bar{p}(x)\gamma^\mu\gamma_5 n(x)F(x-y)\times\int_x^y dz_\nu\int da\mathcal{A}^\nu(z-a)F(a)\partial_\mu\pi^+(y). \tag{24}$$

The additional interaction is important to get the renormalized proton (neutron) charge 1 (0). It can be expressed in momentum space as

$$\mathcal{L}^{\rm add} = e\int\frac{d^4p'}{(2\pi)^4}\int\frac{d^4p}{(2\pi)^4}\int\frac{d^4k}{(2\pi)^4}\int\frac{d^4k_1}{(2\pi)^4}\times\frac{D+F}{\sqrt{2}f}\bar{p}(p')\not{k}\gamma_5 n(p)\tilde{F}(k_1)\tilde{I}\times(p'-p-k_1,k_1-k)\pi^+(k), \tag{25}$$

where $\tilde{I}(p_1,p_2)$ is the Fourier transformation of $I(x,y)$ and the path p is not shown explicitly here. With Taylor expansion of $\tilde{F}(k_1)$, and then Fourier transforming back to position space, we have

$$\mathcal{L}^{\rm add} = e\int dx\int dy\int dz\frac{d^4k}{(2\pi)^4}\frac{D+F}{\sqrt{2}f}\bar{p}(x)\not{k}\gamma_5 n(x)\pi^+(y)\times\left[\sum_{n=0}^{\infty}\frac{\tilde{F}^n(0)}{n!}(-\partial_z^2)^n I(x,z)\exp(ik(y-z))\right]\delta(x-z). \tag{26}$$

From the above equation, one can see that with Taylor expansion, the interaction is related to the derivatives of the path integral. Therefore one can get the path independent vertex. With tedious differentiation as in Refs. [38,39], the vertex in momentum space is expressed as

$$\Gamma_\mu = -e\frac{D+F}{\sqrt{2}f}\not{k}\gamma_5\tilde{F}(q)\sum_{n=0}^{\infty}\frac{\tilde{F}^n(0)}{n!}(2k+q)_\mu\frac{(k+q)^{2n}-q^{2n}}{q^2+2k\cdot q} = -e\frac{D+F}{\sqrt{2}f}\not{k}\gamma_5\tilde{F}(q)(2k+q)_\mu\frac{\tilde{F}(k+q)-\tilde{F}(q)}{q^2+2k\cdot q}. \tag{27}$$

The Feynman rules for the nonlocal Lagrangian are all listed in the appendix.

III. ELECTROMAGNETIC FORM FACTORS

The Dirac and Pauli form factors are defined as

$$\langle N(p')|J_\mu|N(p)\rangle = \bar{u}(p')\left\{\gamma^\mu F_1^N(Q^2)+\frac{i\sigma^{\mu\nu}q_\nu}{2m_N}F_2^N(Q^2)\right\}u(p), \tag{28}$$

where $q=p'-p$ and $Q^2=-q^2$. $F_1^N(Q^2)$ and $F_2^N(Q^2)$ are the Dirac and Pauli form factors. The combination of the above form factors can generate the electric and magnetic form factors as

$$G_E^N(Q^2) = F_1^N(Q^2)-\frac{Q^2}{4m_N^2}F_2^N(Q^2)$$
$$G_M^N(Q^2) = F_1^N(Q^2)+F_2^N(Q^2). \tag{29}$$

Charge and magnetic radii are defined by

$$\langle (r_E^p)^2\rangle = \frac{-6}{G_E^p(0)}\frac{dG_E^p(Q^2)}{dQ^2}\Big|_{Q^2=0},$$
$$\langle (r_M^p)^2\rangle = \frac{-6}{G_M^p(0)}\frac{dG_M^p(Q^2)}{dQ^2}\Big|_{Q^2=0}, \tag{30}$$

$$\langle (r_E^n)^2\rangle = -6\frac{dG_E^n(Q^2)}{dQ^2}\Big|_{Q^2=0},$$
$$\langle (r_M^n)^2\rangle = \frac{-6}{G_M^n(0)}\frac{dG_M^n(Q^2)}{dQ^2}\Big|_{Q^2=0}. \tag{31}$$

According to the Lagrangian, the one-loop Feynman diagrams that contribute to the nucleon electromagnetic form factors are plotted in Fig. 1.

In this section, we only show the expressions for the intermediate octet baryon part. For the intermediate decuplet baryon part, the expressions are written in the appendix. In diagram Fig. 1(a), the photon couples to the meson. The contribution of Fig. 1(a) to the matrix element in Eq. (28) is expressed as

$$\Gamma_a^{\mu(p)} = -(D+F)^2 I_{a\pi}^N - \frac{(3F+D)^2}{6}I_{aK}^\Lambda - \frac{(D-F)^2}{2}I_{aK}^\Sigma, \tag{32}$$

$$\Gamma_a^{\mu(n)} = (D+F)^2 I_{a\pi}^N - (D-F)^2 I_{aK}^\Sigma, \tag{33}$$

where $I_{a\pi}^N$, I_{aK}^Λ, and I_{aK}^Σ are the integrals for the $N\pi$, ΛK, and ΣK intermediate states, respectively. $I_{a\pi}^N$ is expressed as

$$I_{a\pi}^N = \tilde{F}(q)\bar{u}(p')\int\frac{d^4k}{(2\pi)^4}\frac{(\not{k}+\not{q})\gamma_5}{\sqrt{2}f}\tilde{F}(q+k)\frac{1}{D_\pi(k+q)}(2k+q)^\mu\frac{1}{D_\pi(k)}\frac{1}{\not{p}-\not{k}-m_N}\frac{-\not{k}\gamma_5}{\sqrt{2}f}\tilde{F}(k)u(p). \tag{34}$$

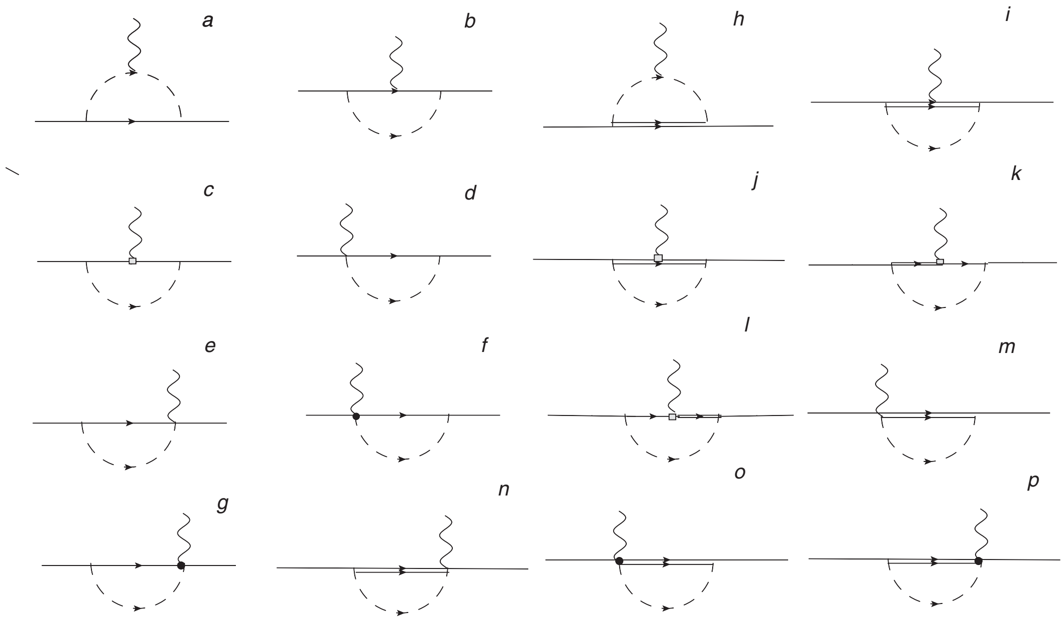

FIG. 1. One-loop Feynman diagrams for the nucleon electromagnetic form factors. The solid, double-solid, dashed, and wave lines are for the octet baryons, decuplet baryons, pseudoscalar mesons, and photons, respectively. The rectangle and black dot represent magnetic and additional interacting vertex.

$D_\pi(k)$ is given by

$$D_\pi(k) = k^2 - M_k^2 + i\epsilon. \tag{35}$$

The expressions for I_{aK}^{Λ} and I_{aK}^{Σ} are the same except the intermediate meson and baryon masses are changed to be those of K meson and hyperons. For simplicity, we only show the expression for the π meson case.

In Fig. 1(b), the photon couples to the intermediate baryon with electric vertex. The contribution of this diagram with octet intermediate baryons is expressed as

$$\begin{aligned}\Gamma_b^{\mu(p)} = {} & \frac{1}{2}(D+F)^2\frac{12m_p^2 - c_1Q^2}{12m_p^2+3Q^2}I_{b\pi}^{NN} \\ & + \frac{(3F-D)^2}{6}\frac{4m_p^2+c_1Q^2}{4m_p^2+Q^2}I_{b\eta}^{NN} + (D-F)^2\frac{24m_\Sigma^2+7c_1Q^2}{24m_\Sigma^2+6Q^2}I_{bK}^{N\Sigma} \\ & - \frac{(3F+D)^2}{18}\frac{c_1Q^2}{4m_\Lambda^2+Q^2}I_{bK}^{N\Lambda} - \frac{(3F+D)(D-F)}{3}\frac{c_1Q^2}{4m_\Sigma^2+Q^2}I_{bK}^{N\Lambda\Sigma},\end{aligned} \tag{36}$$

$$\begin{aligned}\Gamma_b^{\mu(n)} = {} & (D+F)^2\frac{12m_p^2+2c_1Q^2}{12m_p^2+3Q^2}I_{b\pi}^{NN} - \frac{(3F-D)^2}{9}\frac{c_1Q^2}{4m_p^2+Q^2}I_{b\eta}^{NN} - \frac{(3F+D)^2}{18}\frac{c_1Q^2}{4m_\Lambda^2+Q^2}I_{bK}^{N\Lambda} \\ & - (D-F)^2\frac{c_1Q^2+24m_\Sigma^2}{24m_\Sigma^2+6Q^2}I_{bK}^{N\Sigma} + \frac{(3F+D)(D-F)}{3}\frac{c_1Q^2}{4m_\Sigma^2+Q^2}I_{bK}^{N\Lambda\Sigma},\end{aligned} \tag{37}$$

where the integral $I_{b\pi}^{NN}$ is written as

$$I_{b\pi}^{NN} = \tilde{F}(q)\bar{u}(p')\int\frac{d^4k}{(2\pi)^4}\frac{\not{k}\gamma_5}{\sqrt{2}f}\tilde{F}(k)\frac{1}{D_\pi(k)}\frac{1}{\not{p}'-\not{k}-m_N}(-\gamma_\mu)\frac{1}{\not{p}-\not{k}-m_N}\frac{-\not{k}\gamma_5}{\sqrt{2}f}\tilde{F}(k)u(p). \tag{38}$$

Figure 1(c) is for the magnetic baryon-photon interaction. The contribution of this diagram is expressed as

$$\Gamma_c^{\mu(p)} = -\frac{(4c_1+12)m_p^2}{12m_p^2+3Q^2}(D+F)^2 I_{c\pi}^{NN} + \frac{(4c_1-4)m_p^2}{12m_p^2+3Q^2}(3F-D)^2 I_{c\eta}^{NN} - \frac{4c_1 m_\Lambda^2}{36m_\Lambda^2+9Q^2}(3F+D)^2 I_{cK}^{N\Lambda} + \frac{(28c_1-24)m_\Sigma^2}{12m_\Sigma^2+3Q^2}(D-F)^2 I_{cK}^{N\Sigma} - \frac{8c_1(D-F)(3F+D)m_\Sigma^2}{12m_\Sigma^2+3Q^2} I_{cK}^{N\Lambda\Sigma}, \tag{39}$$

$$\Gamma_c^{\mu(n)} = \frac{(16c_1-24)m_p^2}{12m_p^2+3Q^2}(D+F)^2 I_{c\pi}^{NN} - \frac{8c_1 m_N^2}{36m_N^2+9Q^2}(3F-D)^2 I_{c\eta}^{NN} - \frac{4c_1 m_\Lambda^2}{36m_\Lambda^2+9Q^2}(3F+D)^2 I_{cK}^{N\Lambda} - \frac{(4c_1-24)m_\Sigma^2}{12m_\Sigma^2+3Q^2}(D-F)^2 I_{cK}^{N\Sigma} + \frac{8c_1(D-F)(3F+D)m_\Sigma^2}{12m_\Sigma^2+3Q^2} I_{cK}^{N\Lambda\Sigma}, \tag{40}$$

where

$$I_{c\pi}^{NN} = \tilde{F}(q)\bar{u}(p')\int \frac{d^4k}{(2\pi)^4}\frac{\not{k}\gamma_5}{2f}\tilde{F}(k)\frac{1}{\not{p}'-\not{k}-m_N}\frac{\sigma^{\mu\nu}q_\nu}{2m_N}\frac{1}{\not{p}-\not{k}-m_N}\frac{i}{D_\pi(k)}\frac{\not{k}\gamma_5}{2f}\tilde{F}(k)u(p). \tag{41}$$

The contribution from Figs. 1(d) and 1(e) is written as

$$\Gamma_{d+e}^{\mu(p)} = -(D+F)^2 I_{(d+e)\pi}^{NN} - \frac{(3F+D)^2}{6} I_{(d+e)K}^{N\Lambda} - \frac{(D-F)^2}{2} I_{(d+e)K}^{N\Sigma}, \tag{42}$$

$$\Gamma_{d+e}^{\mu(n)} = (D+F)^2 I_{(d+e)\pi}^{NN} - (D-F)^2 I_{(d+e)K}^{N\Sigma}, \tag{43}$$

where

$$I_{(d+e)\pi}^{NN} = \tilde{F}(q)\bar{u}(p')\int \frac{d^4k}{(2\pi)^4}\frac{\not{k}\gamma_5}{\sqrt{2}f}\tilde{F}(k)\frac{1}{\not{p}'-\not{k}-m}\frac{1}{D_\pi(k)}\frac{-1}{\sqrt{2}f}\gamma^\mu\gamma_5\tilde{F}(q-k)u(p) + \tilde{F}(q)\bar{u}(p')\int \frac{d^4k}{(2\pi)^4}\frac{1}{\sqrt{2}f}\gamma^\mu\gamma_5\tilde{F}(q+k)\frac{1}{\not{p}-\not{k}-m}\frac{1}{D_\pi(k)}\frac{-\not{k}\gamma_5}{\sqrt{2}f}\tilde{F}(k)u(p). \tag{44}$$

These two diagrams only have contribution in the relativistic cases. In the heavy baryon limit, they have no contribution to either electric or magnetic form factors.

Figures 1(f) and 1(g) are the additional diagrams that generated from the expansion of the gauge link terms. They are important to get the renormalized charge to proton (neutron) to be 1 (0). The contribution of these two additional diagrams with intermediate octet baryons is expressed as

$$\Gamma_{f+g}^{\mu(p)} = -(D+F)^2 I_{(f+g)\pi}^{NN} - \frac{(3F+D)^2}{6} I_{(f+g)K}^{N\Lambda} - \frac{(D-F)^2}{2} I_{(f+g)K}^{N\Sigma}, \tag{45}$$

$$\Gamma_{f+g}^{\mu(n)} = (D+F)^2 I_{(f+g)\pi}^{NN} - (D-F)^2 I_{(f+g)K}^{N\Sigma}, \tag{46}$$

where

$$I_{(f+g)\pi}^{NN} = \tilde{F}(q)\bar{u}(p')\int \frac{d^4k}{(2\pi)^4}\frac{\not{k}\gamma_5}{\sqrt{2}f}\tilde{F}(k)\frac{1}{\not{p}'-\not{k}-m}\frac{1}{D_\pi(k)}\frac{1}{\sqrt{2}f}(-\not{k}\gamma_5)\frac{(-2k+q)^\mu}{-2kq+q^2}[\tilde{F}(k-q)-\tilde{F}(k)]u(p) + \tilde{F}(q)\bar{u}(p')\int \frac{d^4k}{(2\pi)^4}\frac{1}{\sqrt{2}f}\not{k}\gamma_5\frac{(2k+q)^\mu}{2kq+q^2}[\tilde{F}(k+q)-\tilde{F}(k)]\frac{1}{\not{p}-\not{k}-m}\frac{1}{D_\pi(k)}\frac{\not{k}\gamma_5}{\sqrt{2}f}\tilde{F}(k)u(p). \tag{47}$$

Using FeynCalc to simplify the γ matrix algebra, we can get the separate expressions for the Dirac and Pauli form factors. Numerical results are discussed in the next section.

IV. NUMERICAL RESULTS

In the numerical calculations, the parameters are chosen as $D = 0.76$ and $F = 0.50$ ($g_A = D + F = 1.26$). The coupling constant $\mathcal{C}$ is chosen to be 1 which is the same as in Ref. [41]. The off-shell parameter z is chosen to be $z = -1$ [42]. The low energy constant c_1 is fitted by the experimental moment of $F_2^n(0) = -1.91$. The covariant regulator is chosen to be of a dipole form

$$\tilde{F}(k) = \frac{1}{(1 - k^2/\Lambda^2)^2}, \tag{48}$$

where Lambda is the only free parameter. By varying the value of Λ, we found that when Λ is around 0.85 GeV, the results are very close to the experimental nucleon form factors.

The calculated proton magnetic form factor $G_M^p(Q^2)$ versus Q^2 is plotted in Fig. 2. The solid line is for the empirical result with $G_M^p(Q^2) = 2.79/(1 + Q^2/0.71\ \mathrm{GeV}^2)^2$. The dotted, dot-dashed, and dashed lines are for the tree, loop, and total contribution, respectively. As we explained previously, on the one hand, the nonlocal Lagrangian generates the covariant regulator that makes the loop integral convergent. On the other hand, it also generates the Q^2 dependent contribution at tree level. Compared with the conventional ChPT, the tree level contribution is not expanded in powers of momentum transfer. As a result, both the tree and loop contribution decrease smoothly with the increasing Q^2 and the total obtained form factor is close to the experimental value up to $Q^2 = 2\ \mathrm{GeV}^2$. For $Q^2 = 0$, the contribution to μ_p at tree level is 2.11 and the loop contribution to μ_p is 0.67. The total μ_p is 2.78. This proton magnetic moment is calculated with fixed c_1, which is determined by the neutron magnetic moment ($\mu_n = -1.91$). The proton magnetic radii is 0.848 fm in our calculation, which is obviously close to the experimental value.

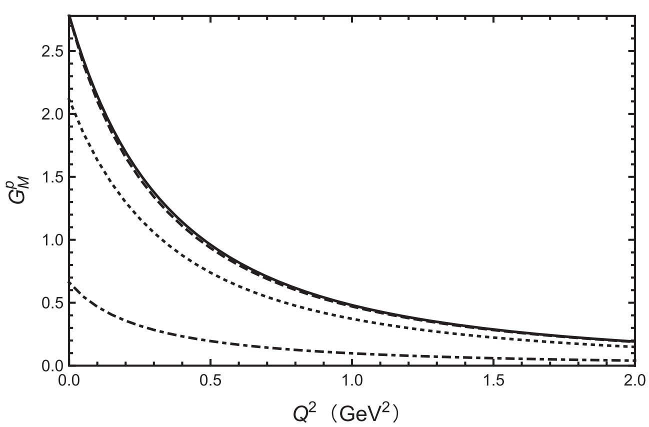

FIG. 2. The proton magnetic form factor versus momentum transfer Q^2 with $\Lambda = 0.85$ GeV. The solid line is for the empirical result. The dotted, dot-dashed, and dashed lines are for the tree, loop, and total contribution, respectively.

The proton charge form factor versus Q^2 is shown in Fig 3. The solid, dashed, dotted, and dot-dashed lines have the same meaning as Fig. 2 except for the charge form factor. From the figure, one can see that both the tree and loop contribution are important to get the correct Q^2 dependence of the form factors. At $Q^2 = 0$, the sum of the tree and loop contribution to proton charge is 1. The additional diagrams generated from the expansion of the gauge link are crucial to get the renormalized proton charge 1. Compared with the magnetic form factor, the charge form factor decreases faster. As a result, the obtained charge radii of 0.857 fm are a little larger than the magnetic radii.

The neutron magnetic form factor versus Q^2 is shown in Fig. 4. Similar as the proton case, the solid line is for the empirical result. The dotted, dot-dashed, and dashed lines represent the tree, loop, and total contribution to the neutron form factor, respectively. Again, compared with the empirical data, our calculated result is very good up to $Q^2 = 2\ \mathrm{GeV}^2$. The calculated magnetic radii of neutron are 0.867 fm. From Figs. 2 to 4, we can see the loop diagrams contribute about 25%–30% to proton electromagnetic form factors and neutron magnetic form factor, while 70%–75% of the form factors is from the tree level contribution.

The neutron charge form factor is plotted in Fig. 5. Since the charge of the neutron is 0, all the contribution to the neutron charge form factor is from the loop. It first increases and then decreases with the increasing momentum transfer. The neutron charge radii $\langle (r_M^n)^2 \rangle = -0.077\ \mathrm{fm}^2$, which is smaller than experimental value $-0.11\ \mathrm{fm}^2$. Though the calculated charge form factor of neutron is smaller than experimental values, overall the result is still reasonable.

In the traditional ChPT, in addition to the two parameters c_1 and c_2 that were determined by the proton and neutron

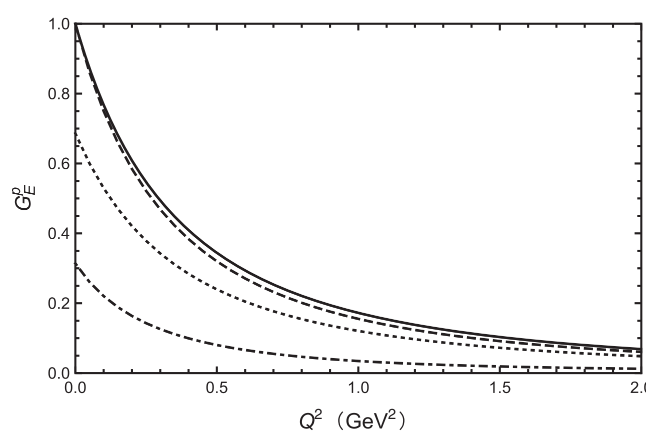

FIG. 3. Same as Fig. 2 but for the proton electric form factor.

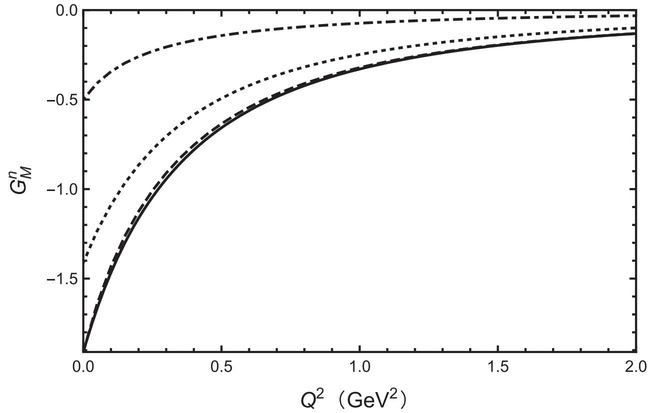

FIG. 4. The magnetic form factor of neutron versus momentum transfer Q^2 with $\Lambda = 0.85$ GeV. The solid line is for the empirical result. The dotted, dot-dashed, and dashed lines are for the tree, loop, and total contribution, respectively.

magnetic moments, there are four other parameters fitted by the electric and magnetic radii of proton and neutron. Here besides the parameter c_1 fitted by the experimental neutron magnetic moment, we have only one free parameter Λ in the regulator. The proton magnetic moment and the nucleon radii are calculated instead of fitted. With fewer parameters, the obtained electromagnetic form factors of proton and neutron are all much better than those in the traditional ChPT. This makes it possible to study the form factors precisely at relatively large Q^2.

With the precisely determined form factors, we now show the ratios of the electric to normalized magnetic form factor. The ratio for the proton is plotted in Fig 6. If without loop contribution, the ratio remains 1 for all Q^2. With loop contribution, $\frac{\mu_p G_E^p}{G_M^p}$ automatically deceases with the increasing Q^2. Our calculated result is comparable with the experimental data, though at large Q^2, the experimental data drop more quickly.

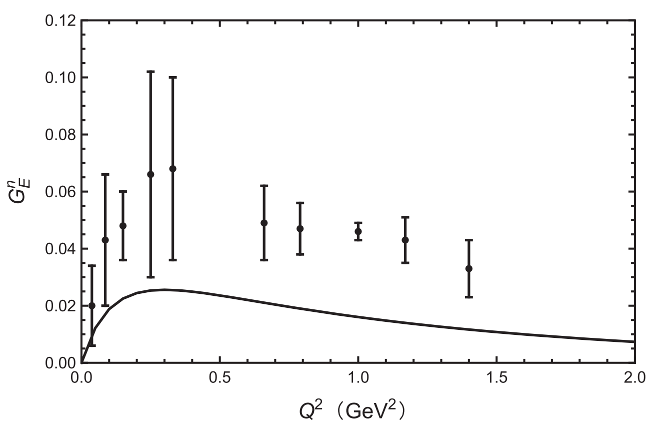

FIG. 5. The electric form factor of neutron versus momentum transfer Q^2 with $\Lambda = 0.85$ GeV. The experimental date are from [43].

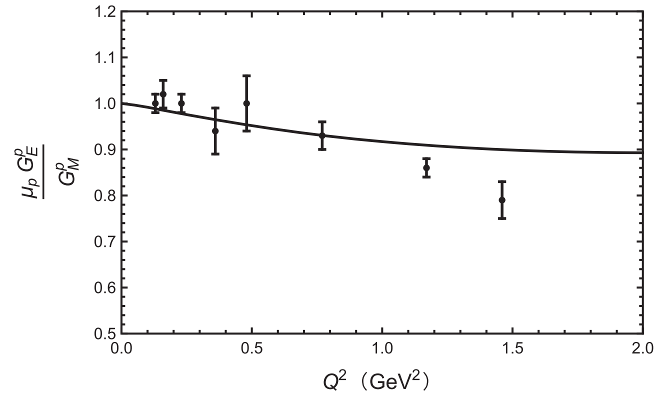

FIG. 6. Radio of proton electric to normalized magnetic form factor versus momentum transfer Q^2. The experimental result is from [44].

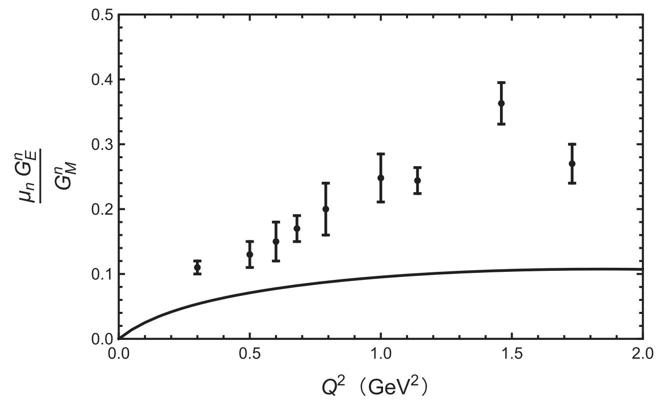

FIG. 7. Radio of neutron electric to normalized magnetic form factor versus momentum transfer Q^2. The experimental result is from [45].

The ratio for neutron is plotted in Fig. 7. From the figure, one can see the ratio $\frac{\mu_n G_E^n}{G_M^n}$ increases with the increasing Q^2 as the experimental data. This is purely due to the loop contribution. The experimental ratio of $\frac{\mu_n G_E^n}{G_M^n}$ increases more quickly than our result. It is mainly because our calculated G_E^n is smaller than the experimental data.

V. SUMMARY

We proposed a relativistic version for the finite-range regularization that makes it possible to study the hadron properties with relativistic chiral effective Lagrangian at large Q^2. The finite-range regularization has been widely applied to investigate the nucleon mass, form factors, electromagnetic radii, generalized parton distributions, proton spin, etc. We have good knowledge on the three-dimensional regulator that was kept the same for all the calculations. However, we have little knowledge on the covariant four-dimensional regulator. Therefore, we start from the well-determined nucleon form factors and it was found that using the dipole regulator with Λ around

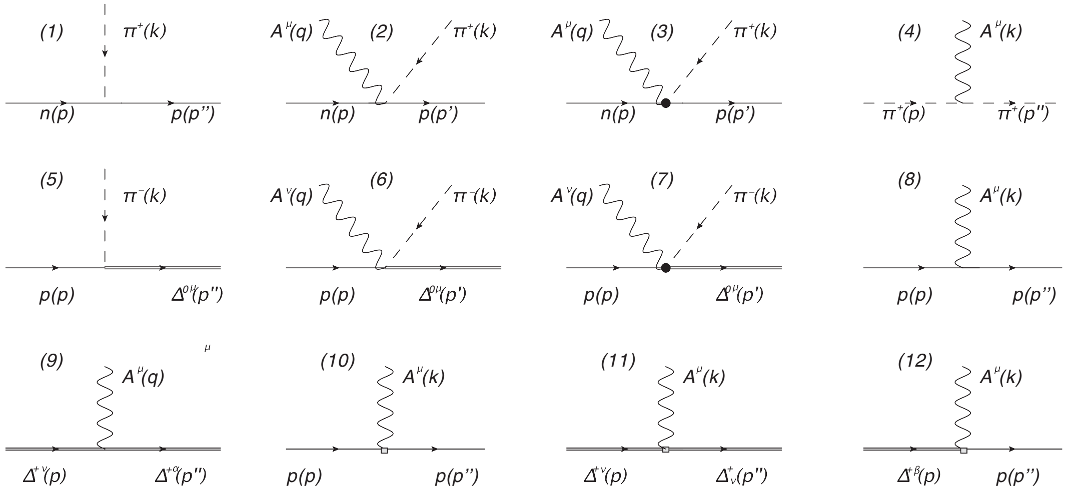

FIG. 8. The interacting vertex in the calculation of nucleon form factors. Only the π case is shown as an example. The rectangle and black dot represent the magnetic and additional interacting vertex.

0.85 GeV the nucleon form factors can be described very well up to $Q^2 = 2\ \mathrm{GeV}^2$. The covariant regulator is generated from the nonlocal gauge invariant Lagrangian. As a result, the renormalized charge of proton (neutron) is 1 (0) with the additional diagrams obtained by the expansion of the gauge link. The nonlocal interaction generates both the regulator, which makes the loop integral convergent, and the Q^2 dependence of form factors at tree level. In this approach, we have only two parameters c_1 and Λ instead of six parameters in the traditional ChPT. With fewer parameters, our calculated form factors are much better. The ratios of the electric to normalized magnetic form factor are also comparable with the experimental data. From our calculation, the G_N^E/G_N^M puzzle can be naturally understood. This is the first time that we calculate the form factors precisely at relatively large Q^2 with chiral effective Lagrangian. The successful application of chiral effective Lagrangian to large momentum transfer is very helpful for us to investigate hadron quantities at high Q^2. As a summary, we list the parameters and obtained magnetic moments and electromagnetic radii in Table I.

ACKNOWLEDGMENTS

This work is supported by NSFC under Grant No. 11475186, by DFG and NSFC (CRC 110), and by Key Research Program of Frontier Sciences, CAS under Grant No. Y7292610K1.

TABLE I. The parameters and calculated magnetic moments and electromagnetic radii of nucleon.

Λ (GeV)	Z	c_1	μ_p	μ_n	r_{Mp} (fm)	r_{Ep} (fm)	r_{Mn} (fm)	r_{En}^2 (fm^2)
0.8	0.71	3.090	2.78	−1.91	0.893	0.903	0.912	−0.076
0.85	0.69	3.085	2.78	−1.91	0.848	0.857	0.867	−0.077
0.9	0.66	3.077	2.78	−1.91	0.808	0.816	0.829	−0.082
Exp.	⋯	⋯	2.79	−1.91	0.836	0.847	0.889	−0.113

APPENDIX: FEYNMAN RULES AND DECUPLET CONTRIBUTION

The Feynman rules for the nonlocal vertices plotted in Fig. 8 are written as written as

$$(1):\ \frac{\not{k}\gamma_5}{\sqrt{2}f}(D+F)\tilde{F}(k)$$

$$(2):\ -\frac{e}{\sqrt{2}f}(D+F)\gamma^\mu\gamma_5\tilde{F}(k+q)\tilde{F}(q)$$

$$(3):\ -\frac{e}{\sqrt{2}f}(D+F)\not{k}\gamma_5\frac{(2k+q)^\mu}{2kq+q^2}[\tilde{F}(k+q)-\tilde{F}(k)]\tilde{F}(q)$$

$$(4):\ -ie(p+p'')^\mu\tilde{F}(q)$$

$$(5):\ -\frac{\mathcal{C}}{\sqrt{6}f}(k_\mu+z\gamma_\mu\not{k})\tilde{F}(k)$$

$$(6):\ -\frac{e\mathcal{C}}{\sqrt{6}f}(g^{\nu\mu}+z\gamma^\mu\gamma^\nu)\tilde{F}(k+q)\tilde{F}(q)$$

$$(7):\ -\frac{e\mathcal{C}}{\sqrt{6}f}(k_\mu+z\gamma_\mu\not{k})\frac{(2k+q)^\mu}{2kq+q^2}[\tilde{F}(k+q)-\tilde{F}(k)]\tilde{F}(q)$$

$$(8):\ -ie\gamma^\mu\frac{4m_N^2+c_1Q^2}{4m_N^2+Q^2}\tilde{F}(q)$$

$$(9):\ -ie\gamma^{\alpha\nu\mu}\frac{4m_\Delta^2+c_1Q^2}{4m_\Delta^2+Q^2}\tilde{F}(q)$$

$$(10):\ \frac{4e(c_1-1)m_N^2}{4m_N^2+Q^2}\frac{\sigma^{\mu\nu}q_\nu}{2m_N}\tilde{F}(q)$$

$$(11):\ -\frac{4e(c_1-1)m_\Delta^2}{4m_\Delta^2+Q^2}\frac{\sigma^{\mu\lambda}q_\lambda}{2m_\Delta}\tilde{F}(q)$$

$$(12):\ e\frac{\sqrt{3}}{3m_N}c_1F_{\mu\nu}\gamma^\mu\gamma_5\tilde{F}(q).$$

The expressions for the decuplet part are written in the following way. The contribution of Fig. 1(h) is expressed as

$$\Gamma_h^{\mu(p)} = \frac{2\mathcal{C}^2}{3} I_{h\pi}^{N\Delta} - \frac{\mathcal{C}^2}{6} I_{hK}^{N\Sigma^*}, \tag{A1}$$

$$\Gamma_h^{\mu(n)} = -\frac{2\mathcal{C}^2}{3} I_{h\pi}^{N\Delta} - \frac{\mathcal{C}^2}{3} I_{hK}^{N\Sigma^*}, \tag{A2}$$

where

$$\begin{aligned} I_{h\pi}^{N\Delta} = {}& \tilde{F}(q)\bar{u}(p') \int \frac{d^4k}{(2\pi)^4} \frac{1}{2f^2} ((k+q)_\sigma \\ & + z(\not{k}+\not{q})\gamma_\sigma))\tilde{F}(q+k)\frac{1}{D_\pi(k+q)} \\ & \times e(2k+q)^\mu \frac{1}{D_\pi(k)} \frac{1}{\not{p}-\not{k}-m_\Delta} \\ & \times S_{\sigma\rho}(-k_\rho - z\gamma_\rho\not{k})\tilde{F}(k)u(p). \end{aligned} \tag{A3}$$

$S_{\sigma\rho}$ is expressed as

$$\begin{aligned} S_{\sigma\rho} = {}& -g_{\sigma\rho} + \frac{\gamma_\sigma\gamma_\rho}{3} + \frac{2(p-k)_\sigma(p-k)_\rho}{3m_\Delta^2} \\ & + \frac{\gamma_\sigma(p-k)_\rho - \gamma_\rho(p-k)_\sigma}{3m_\Delta}. \end{aligned} \tag{A4}$$

The contribution of Fig. 1(i) is expressed as

$$\Gamma_i^{\mu(p)} = \frac{4\mathcal{C}^2}{3}\frac{4m_\Delta^2+c_1Q^2}{4m_\Delta^2+Q^2} I_{i\pi}^{N\Delta} + \frac{\mathcal{C}^2}{6}\frac{4m_\Sigma^{*2}+c_1Q^2}{4m_\Sigma^{*2}+Q^2} I_{iK}^{N\Sigma^*}, \tag{A5}$$

$$\Gamma_i^{\mu(n)} = -\frac{\mathcal{C}^2}{3}\frac{4m_\Delta^2+c_1Q^2}{4m_\Delta^2+Q^2} I_{i\pi}^{N\Delta} - \frac{\mathcal{C}^2}{6}\frac{4m_\Sigma^{*2}+c_1Q^2}{4m_\Sigma^{*2}+Q^2} I_{iK}^{N\Sigma^*}, \tag{A6}$$

where

$$\begin{aligned} I_{i\pi}^{N\Delta} = {}& \tilde{F}(q)\bar{u}(p') \int \frac{d^4k}{(2\pi)^4} \frac{1}{2f^2} (k_\sigma + z\not{k}\gamma_\sigma)\tilde{F}(k)\frac{1}{D_\pi(k)} \\ & \times \frac{1}{\not{p}'-\not{k}-m_\Delta} S_{\sigma\alpha} \times (-2\gamma^{\alpha\beta\mu}) \frac{1}{\not{p}-\not{k}-m_\Delta} \\ & \times S_{\beta\rho}(-k_\rho - z\gamma_\rho\not{k})\tilde{F}(k)u(p). \end{aligned} \tag{A7}$$

The contribution of Fig. 1(j) is expressed as

$$\Gamma_j^{\mu(p)} = \frac{4\mathcal{C}^2}{3}\frac{4m_\Delta^2}{4m_\Delta^2+Q^2} I_{j\pi}^{N\Delta} + \frac{\mathcal{C}^2}{6}\frac{4m_\Sigma^{*2}}{4m_\Sigma^{*2}+Q^2} I_{jK}^{N\Sigma^*}, \tag{A8}$$

$$\Gamma_j^{\mu(n)} = -\frac{\mathcal{C}^2}{3}\frac{4m_\Delta^2}{4m_\Delta^2+Q^2} I_{j\pi}^{N\Delta} - \frac{\mathcal{C}^2}{6}\frac{4m_\Sigma^{*2}}{4m_\Sigma^{*2}+Q^2} I_{jK}^{N\Sigma^*}, \tag{A9}$$

where

$$\begin{aligned} I_{j\pi}^{N\Delta} = {}& \tilde{F}(q)\bar{u}(p') \int \frac{d^4k}{(2\pi)^4} \frac{1}{2f^2} (k_\sigma + z\not{k}\gamma_\sigma)\tilde{F}(k)\frac{i}{D_\pi(k)} \frac{i}{\not{p}'-\not{k}-m_\Delta} S_{\sigma\nu}\frac{(1-c_1)}{m_\Delta}\sigma^{\mu\lambda}q_\lambda \\ & \times \frac{i}{\not{p}-\not{k}-m_\Delta} S_{\nu\rho}(-k_\rho - z\gamma_\rho\not{k})\tilde{F}(k)u(p). \end{aligned} \tag{A10}$$

The contribution of Figs. 1(k) and 1(l) is expressed as

$$\Gamma_{k+l}^{\mu(p)} = 2(D+F)\mathcal{C}I_{(k+l)\pi}^{N\Delta} + \frac{5}{4}(D-F)\mathcal{C}I_{(k+l)K}^{\Sigma\Sigma^*} + \frac{1}{4}(3F+D)\mathcal{C}I_{(k+l)K}^{\Lambda\Sigma^*}, \tag{A11}$$

$$\Gamma_{k+l}^{\mu(n)} = -2(D+F)\mathcal{C}I_{(k+l)\pi}^{N\Delta} + \frac{1}{4}(D+F)\mathcal{C}I_{(k+l)K}^{\Sigma\Sigma^*} - \frac{1}{4}(3F+D)\mathcal{C}I_{(k+l)K}^{\Lambda\Sigma^*}, \tag{A12}$$

where

$$\begin{aligned} I_{(k+l)\pi}^{\Sigma\Sigma^*} = {}& -\tilde{F}(q)\bar{u}(p') \int \frac{d^4k}{(2\pi)^4} \frac{c_1}{6m_{\Sigma^*}f^2} \tilde{F}^2(k)\not{k}\gamma_5 \frac{1}{\not{p}'-\not{k}-m_\Sigma} \gamma^\nu\gamma_5 q_\nu \frac{1}{\not{p}-\not{k}-m_{\Sigma^*}} S_{\mu\rho}(k_\rho + z\gamma_\rho\not{k})\frac{i}{D_\pi(k)} u(p) \\ & + \tilde{F}(q)\bar{u}(p') \int \frac{d^4k}{(2\pi)^4} \frac{c_1}{6m_{\Sigma^*}f^2} \tilde{F}^2(k)\not{k}\gamma_5 \frac{1}{\not{p}'-\not{k}-m_\Sigma} \gamma^\mu\gamma_5 q_\nu \frac{1}{\not{p}-\not{k}-m_{\Sigma^*}} S_{\nu\rho}(k_\rho + z\gamma_\rho\not{k})\frac{i}{D_\pi(k)} u(p) \\ & - \tilde{F}(q)\bar{u}(p') \int \frac{d^4k}{(2\pi)^4} \frac{c_1}{6m_{\Sigma^*}f^2} \tilde{F}^2(k)(k_\nu + z\not{k}\gamma_\nu) \frac{1}{\not{p}'-\not{k}-m_\Sigma} S_{\nu\rho}q_\rho\gamma^\mu\gamma_5 \frac{1}{\not{p}-\not{k}-m_{\Sigma^*}} \not{k}\gamma_5 \frac{1}{D_\pi(k)} u(p) \\ & + \tilde{F}(q)\bar{u}(p') \int \frac{d^4k}{(2\pi)^4} \frac{c_1}{6m_{\Sigma^*}f^2} \tilde{F}^2(k)(k_\nu + z\not{k}\gamma_\nu) \frac{1}{\not{p}'-\not{k}-m_\Sigma} S_{\nu\mu}q_\rho\gamma^\rho\gamma_5 \frac{1}{\not{p}-\not{k}-m_{\Sigma^*}} \not{k}\gamma_5 \frac{1}{D_\pi(k)} u(p). \end{aligned} \tag{A13}$$

The contribution of Figs. 1(m) and 1(n) is expressed as

$$\Gamma^{\mu(p)}_{m+n} = \frac{2\mathcal{C}^2}{3} I^{N\Delta}_{(m+n)\pi} - \frac{\mathcal{C}^2}{6} I^{N\Sigma^*}_{(m+n)K}, \tag{A14}$$

$$\Gamma^{\mu(n)}_{m+n} = -\frac{2\mathcal{C}^2}{3} I^{N\Delta}_{(m+n)\pi} - \frac{\mathcal{C}^2}{3} I^{N\Sigma^*}_{(m+n)K}, \tag{A15}$$

where

$$\begin{aligned} I^{N\Delta}_{(m+n)\pi} &= e\tilde{F}(q)\bar{u}(p') \int \frac{d^4k}{(2\pi)^4} \frac{1}{2f^2} (k_\sigma + z\not{k}\gamma_\sigma)\tilde{F}(k) \frac{1}{D_\pi(k)} \frac{1}{\not{p}' - \not{k} - m_\Delta} S_{\sigma\rho}(g^{\rho\mu} + z\gamma^\rho\gamma^\mu)\tilde{F}(-k+q)u(p) \\ &\quad + e\tilde{F}(q)\bar{u}(p') \int \frac{d^4k}{(2\pi)^4} \frac{1}{2f^2} (g^{\sigma\mu} + z\gamma^\mu\gamma^\sigma)\tilde{F}(k+q) \frac{1}{D_\pi(k)} \frac{1}{\not{p} - \not{k} - m_\Delta} S_{\sigma\rho}\tilde{F}(k)(k_\rho + z\gamma_\rho\not{k})u(p). \end{aligned} \tag{A16}$$

The contribution of Figs. 1(o) and 1(p) is expressed as

$$\Gamma^{\mu(p)}_{o+p} = \frac{2\mathcal{C}^2}{3} I^{N\Delta}_{(o+p)\pi} - \frac{\mathcal{C}^2}{6} I^{N\Sigma^*}_{(o+p)K}, \tag{A17}$$

$$\Gamma^{\mu(n)}_{o+p} = -\frac{2\mathcal{C}^2}{3} I^{N\Delta}_{(o+p)\pi} - \frac{\mathcal{C}^2}{3} I^{N\Sigma^*}_{(o+p)K}, \tag{A18}$$

where

$$\begin{aligned} I^{N\Delta}_{(o+p)\pi} &= -e\tilde{F}(q)\bar{u}(p') \int \frac{d^4k}{(2\pi)^4} \frac{1}{2f^2} (k_\sigma + z\not{k}\gamma_\sigma)\tilde{F}(k) \frac{1}{D_\pi(k)} \frac{1}{\not{p}' - \not{k} - m_\Delta} S_{\sigma\rho}(k_\rho + z\gamma_\rho\not{k}) \\ &\quad \times \frac{(-2k+q)^\mu}{-2kq + q^2} [\tilde{F}(k-q) - \tilde{F}(k)]u(p) \\ &\quad + e\tilde{F}(q)\bar{u}(p') \int \frac{d^4k}{(2\pi)^4} \frac{1}{2f^2} (k_\sigma + z\not{k}\gamma_\sigma) \frac{(2k+q)^\mu}{2kq + q^2} [\tilde{F}(k+q) - \tilde{F}(k)] \\ &\quad \times \frac{1}{D_\pi(k)} \frac{1}{\not{p} - \not{k} - m_\Delta} S_{\sigma\rho}\tilde{F}(k)(k_\rho + z\gamma_\rho\not{k})u(p). \end{aligned} \tag{A19}$$

[1] D.-H. Lu, A. W. Thomas, and A. G. Williams, Phys. Rev. C **57**, 2628 (1998).
[2] K. Berger, R. F. Wagenbrunn, and W. Plessas, Phys. Rev. D **70**, 094027 (2004).
[3] B. Julia-Diaz, D. O. Riska, and F. Coester, Phys. Rev. C **69**, 035212 (2004); **75**, 069902(E) (2007).
[4] A. J. Buchmann and R. F. Lebed, Phys. Rev. D **67**, 016002 (2003).
[5] S. Cheedket, V. E. Lyubovitskij, T. Gutsche, A. Faessler, K. Pumsa-ard, and Y. Yan, Eur. Phys. J. A **20**, 317 (2004).
[6] R. A. Williams and C. Puckett-Truman, Phys. Rev. C **53**, 1580 (1996).
[7] P.-N. Shen, Y.-B. Dong, Z.-Y. Zhang, Y.-W. Yu, and T. S. H. Lee, Phys. Rev. C **55**, 2024 (1997).
[8] R. Jakob, P. Kroll, M. Schurmann, and W. Schweiger, Z. Phys. A **347**, 109 (1993).
[9] G. Hellstern and C. Weiss, Phys. Lett. B **351**, 64 (1995).
[10] J. M. Zanotti, D. B. Leinweber, A. G. Williams, and J. B. Zhang, Nucl. Phys. B, Proc. Suppl. **129–130**, 287 (2004).
[11] S. Boinepalli, D. B. Leinweber, A. G. Williams, J. M. Zanotti, and J. B. Zhang, Phys. Rev. D **74**, 093005 (2006).
[12] C. Alexandrou, G. Koutsou, J. W. Negele, and A. Tsapalis, Phys. Rev. D **74**, 034508 (2006).
[13] M. Gockeler, T. R. Hemmert, R. Horsley, D. Pleiter, P. E. L. Rakow, A. Schafer, and G. Schierholz (QCDSF Collaboration), Phys. Rev. D **71**, 034508 (2005).
[14] M. Gockeler *et al.* (QCDSF/UKQCD Collaboration), *Proc. Sci.*, LAT20072007 (2007) 161 [arXiv:0710.2159].
[15] R. G. Edwards, G. T. Fleming, P. Hagler, J. W. Negele, K. Orginos, A. V. Pochinsky, D. B. Renner, D. G. Richards, and W. Schroers (LHPC Collaboration), *Proc. Sci.*, LAT20052006 (2006) 056 [arXiv:0509185].
[16] C. Alexandrou *et al.* (Lattice Hadron Collaboration), J. Phys. Conf. Ser. **16**, 174 (2005).

[17] T. Fuchs, J. Gegelia, and S. Scherer, J. Phys. G **30**, 1407 (2004).
[18] B. Kubis and U.-G. Meissner, Nucl. Phys. **A679**, 698 (2001).
[19] R. D. Young, D. B. Leinweber, and A. W. Thomas, Prog. Part. Nucl. Phys. **50**, 399 (2003).
[20] D. B. Leinweber, A. W. Thomas, and R. D. Young, Phys. Rev. Lett. **92**, 242002 (2004).
[21] P. Wang, D. B. Leinweber, A. W. Thomas, and R. D. Young, Phys. Rev. D **75**, 073012 (2007).
[22] P. Wang and A. W. Thomas, Phys. Rev. D **81**, 114015 (2010).
[23] C. R. Allton, W. Armour, D. B. Leinweber, A. W. Thomas, and R. D. Young, Phys. Lett. B **628**, 125 (2005).
[24] W. Armour, C. R. Allton, D. B. Leinweber, A. W. Thomas, and R. D. Young, Nucl. Phys. **A840**, 97 (2010).
[25] J. M. M. Hall, D. B. Leinweber, and R. D. Young, Phys. Rev. D **88**, 014504 (2013).
[26] D. B. Leinweber, S. Boinepalli, I. C. Cloet, A. W. Thomas, A. G. Williams, R. D. Young, J. M. Zanotti, and J. B. Zhang, Phys. Rev. Lett. **94**, 212001 (2005).
[27] P. Wang, D. B. Leinweber, A. W. Thomas, and R. D. Young, Phys. Rev. C **79**, 065202 (2009).
[28] P. Wang, D. B. Leinweber, A. W. Thomas, and R. D. Young, Phys. Rev. D **86**, 094038 (2012).
[29] P. Wang, D. B. Leinweber, and A. W. Thomas, Phys. Rev. D **89**, 033008 (2014).
[30] J. M. M. Hall, D. B. Leinweber, and R. D. Young, Phys. Rev. D **89**, 054511 (2014).
[31] P. Wang, D. B. Leinweber, and A. W. Thomas, Phys. Rev. D **92**, 034508 (2015).
[32] H. Li, P. Wang, D. B. Leinweber, and A. W. Thomas, Phys. Rev. C **93**, 045203 (2016).
[33] H. Li and P. Wang, Chin. Phys. C **40**, 123106 (2016).
[34] P. Wang, D. B. Leinweber, A. W. Thomas, and R. D. Young, Phys. Rev. D **79**, 094001 (2009).
[35] E. E. Jenkins, Nucl. Phys. **B368**, 190 (1992).
[36] E. E. Jenkins, M. E. Luke, A. V. Manohar, and M. J. Savage, Phys. Lett. B **302**, 482 (1993); **388**, 866(E) (1996).
[37] S. Scherer, Adv. Nucl. Phys. **27**, 277 (2003).
[38] J. Terning, Phys. Rev. D **44**, 887 (1991).
[39] A. Faessler, T. Gutsche, M. A. Ivanov, V. E. Lyubovitskij, and P. Wang, Phys. Rev. D **68**, 014011 (2003).
[40] P. Wang, Can. J. Phys. **92**, 25 (2014).
[41] V. Pascalutsa, M. Vanderhaeghen, and S. N. Yang, Phys. Rep. **437**, 125 (2007).
[42] L. M. Nath, B. Etemadi, and J. D. Kimel, Phys. Rev. D **3**, 2153 (1971).
[43] M. Seimetz (A1 Collaboration), Nucl. Phys. **A755**, 253 (2005).
[44] M. Ostrick, Eur. Phys. J. A **28**, 81 (2006).
[45] S. Riordan *et al.*, Phys. Rev. Lett. **105**, 262302 (2010).